Contact Faces of Epitaxially Crystallized α- and γ-Phase Isotactic Polypropylene Observed by Atomic Force Microscopy

W. Stocker, S. N. Magonov, and H.-J. Cantow

Freiburger Material Forschungszentrum and Institut für Makromolekulare Chemie, Stefan-Maier-Strasse 31, 79104 Freiburg im Breisgau, Federal Republic of Germany

J. C. Wittmann and B. Lotz*

Institut Charles Sadron (CRM-EAHP), CNRS-ULP, 6 rue Boussingault, 67083 Strasbourg Cêdex, France

Received March 31, 1993•

ABSTRACT: The structure and contact faces of epitaxially crystallized isotactic polypropylene (iPP) in its α and γ phases are investigated by electron microscopy, electron diffraction, and atomic force microscopy (AFM). AFM results with methyl group resolution help recognize which one of two possible contact faces interacts with the substrate. Structural analysis makes it possible (at least in the α phase) to determine the hand of helices in contact with the substrate.

Introduction

The resolution reached by near-field microscopy[1] makes it a new and valuable tool to investigate materials surfaces. In the field of crystalline polymers, atomic force microscopy (AFM) reaches methyl group resolution: unfiltered images of paraffin crystals reveal conclusively the pattern of methyl end chains.[2]

The demonstrated ability of AFM to reveal methyl groups has been the trigger for a further investigation of the contact surfaces of isotactic polypropylene (iPP) epitaxially crystallized on low molecular weight organic substrates.[3] For both epitaxially crystallized α– and γ–phase iPP, electron diffraction investigations provide a wealth of information on relative polymer–substrate organization, fold surfaces, crystallographic planes involved in the epitaxy, and even chirality of the constituent helices. Electron diffraction *does not provide one last piece of information: it cannot determine which one of two possible alternate crystallographic planes is actually in contact with the substrate.* Since these possible planes differ by the density and pattern of methyl side chains of iPP, AFM of the actual surfaces should help clarify this issue.

This paper presents in some detail the structure determination, through concerted use of electron microscopy (EM), electron diffraction (ED), and AFM techniques, of epitaxially crystallized α- and γ-phase iPP. Most of the EM and ED work is available, but fragmented in different papers.[3-6] Our AFM results on the α phase of iPP have been briefly presented elsewhere[7] and have been the subject of a short review paper.[8] As will become apparent, AFM gives an unambiguous answer about the nature of the contact surface and therefore provides a truly original insight into details of the epitaxial interactions that are beyond reach of EM and ED techniques.

Experimental Section

1. Materials and Sample Preparation. The substrate materials, mainly benzoic acid and nicotinic acid, are of commercial origin. The iPP sample used was provided by SNEA(P). It has 96% isotactic triads and its molecular weight is 3.8×10^3 with polydispersity = 5.2 Its crystallization characteristics are described elsewhere.[9-12]

Production of pure α phase or of mixed α and γ phases depends mainly on the molecular characteristics of the polymer. The original high molecular weight sample is used to obtain α phase although its crystallization range[9,10] is somewhat high for benzoic acid (T_m = 122 °C). For this reason nicotinic acid (T_m = 234 °C) was also used as a substrate.

γ phase crystallization is favored when low molecular weight material is used. The latter is produced by thermal cracking of the original sample by heating in a molybdenum boat in a bell jar at 10^{-5} Torr. In the process, iPP vapors of MW $\simeq$ 3000[13] condense on the cover slides used for further sample preparation.

Epitaxy of isotactic polypropylene on benzoic or nicotinic acid substrates produces thin films used for EM and AFM investigation. The films are obtained by comelting the polymer and acid between cover glasses and crystallized by sliding on a Kofler hot bench. After separation of the cover slides, the acid is dissolved in ethanol. The remaining thin film is suitable without further processing for AFM examination. Electron microscopic examination requires further steps: optional shadowing with Pt/C pellets at oblique incidence or gold decoration under normal incidence to reveal lamellar structure followed by backing with a carbon film, floating on water (most usually with the help of an additional poly(acrylic acid) backing film), and mounting on copper grids. *In both EM and AFM studies, the contact surface is visualized*: i.e., the epitaxially formed thin film is "looked at" from the viewpoint of the (by now dissolved) substrate.

2. Experimental Techniques. Electron Microscopy. All observations are made with Hitachi HU11CS and Philips CM12 electron microscopes. Electron diffraction patterns are most often recorded on daylight film (400 or 200 ASA).

Atomic Force Microscopy (AFM). AFM experiments are carried out with a Nanoscope II microscope (Digital Instruments, Inc., Santa Barbara, CA) where the tip motion is followed by deflection of a laser beam reflected off the rear side of the cantilever. The deflection is monitored with a position-sensitive detector. All AFM images (morphology and molecular structure) are taken with an A-type scan head (scan range: 700×700 nm^2). Si_3N_4 tips attached to a microfabricated cantilever (200 μm, triangular base) are used. The force constant of the cantilever is small: 0.12 N/m. For distance calibration of the piezo controller, HOPG images with atomic resolution are used. The iPP samples prepared on microscope cover glasses are installed on the stage with the aid of an optical microscope, the tip being positioned close to the surface of preselected flat oriented regions.

The measurements are carried out in the constant force mode in which the deflection of the lever is kept constant by means of a feedback loop. The loop output yields an accurate measure of the motion of the z-piezo (height imaging). The images are recorded in the repulsive region of the force–distance curve, where

* To whom correspondence should be addressed.

• Abstract published in *Advance ACS Abstracts*, September 15, 1993.

0024-9297/93/2226-5915$04.00/0

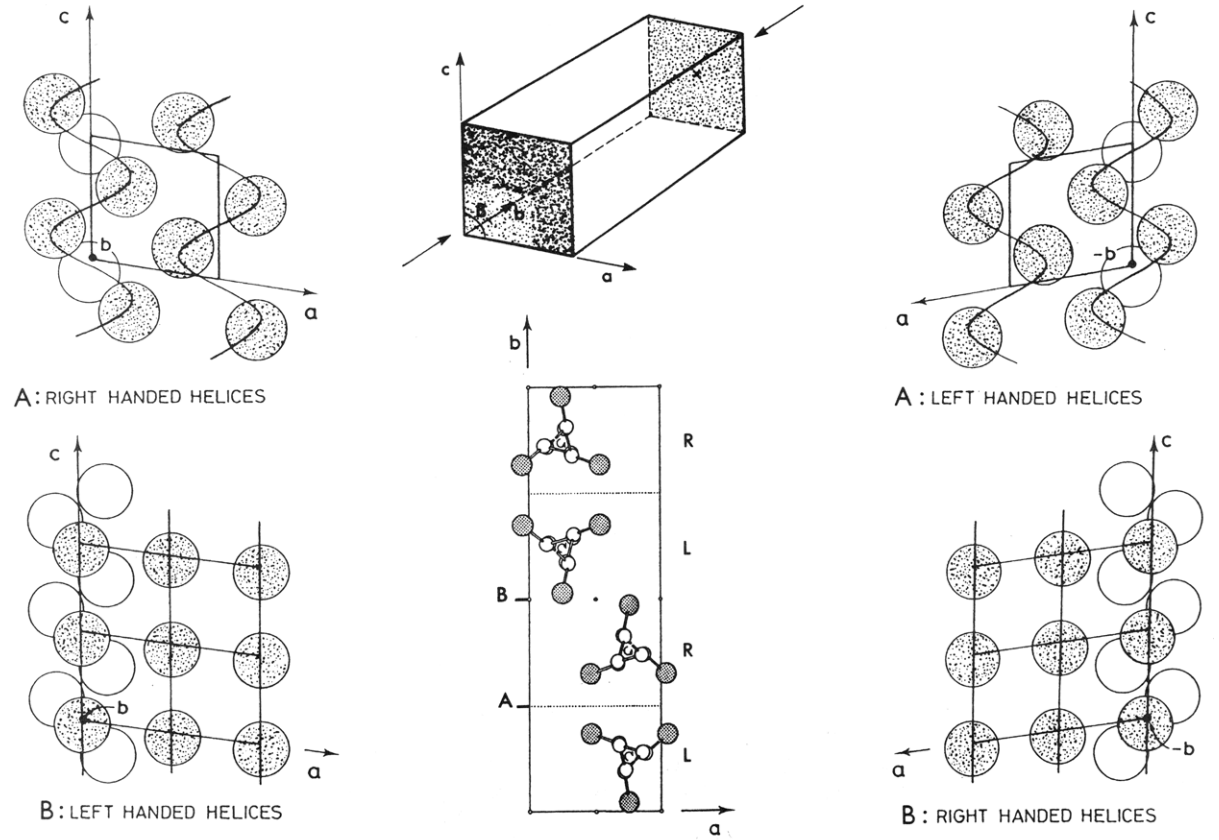

Figure 1. Crystal structure of α-iPP and (010) contact planes. Center bottom: Crystal structure seen in c-axis projection.[13] Note the alteration of right (R) and left (L) hands of helices along the b axis and different azimuthal setting of chains leading to two different contact faces, marked A and B. Contact faces A and B as seen along the $+b$- and $-b$-axis directions (cf. center top) are shown in the left and right of the figure, respectively. Exposed methyl groups are shaded and buried ones are unshaded in only one of the helices shown.

the probing tip is brought into repulsive contact with the sample and the static deflections of the cantilever are measured. Scanning line frequencies are 1 Hz for large-scale scans and up to 39 Hz for smaller areas (10×10 nm^2). In most experiments, images are taken repeatedly by varying the scanning direction over the sample by 30° increments over 180°. This procedure helps verify the observed structure and optimize the scan parameters and quality of recorded images.

For the filtering of recorded AFM images, two-dimensional fast Fourier transformation (2D-FFT) is applied. The strongest frequency patterns of the 2D-FFT are used for image processing, which help determine more accurately lattice spacings of periodic structures.

The Structural Problem

The major characteristics of the iPP α- and γ-phase crystal structures are first restated in the context of the "structure of contact face" issue mentioned in the Introduction. The work described here requires indeed a clear perception of helical hand in the bulk of the crystal structure and in the contact faces of the α and γ phases.

The α-phase crystal structure of isotactic polypropylene is well established.[14-16] It is based on ternary helices with 6.5-Å chain axis repeat distances. Packing of these helices in the monoclinic unit cell of parameters $a = 6.65$ Å, $b = 20.78$ Å, $c = 6.50$ Å, and $\beta = 99.6°$ follows a pattern also observed in several polyolefins (polybutene-1, phase I′, and 1,2 isotactic polybutadiene[17]): the nearest neighbor helices to any one helix are antichiral to it, and the overall organization is such that *isochiral helices are arranged in layers*—in iPP α phase, parallel to the *ac* plane (cf. Figure 1). Furthermore, the azimuthal setting of helices is rotated by 180° for successive layers. These structural features result in four lateral (010) faces which differ by their helical hand and pattern of exposed methyl groups. They are shown in Figure 1, as seen along the $+b$- and $-b$-axis direction on the left- and right-hand side of the figure, respectively. They are characterized by the observation viewpoint, i.e., $+b$- or $-b$-axis direction (the two viewpoints are easily recognized by the dip and right or left orientation of the a-axis direction relative to the c axis (vertical in Figure 1)), and the pattern of methyl groups. If successive methyl groups of a helix turn in right-handed helices are numbered 1, 2, and 3 and methyl groups 2 and 3 are exposed when observed along the $+b$ direction, then the remaining group 1 alone is exposed when observed along the $-b$ direction. These faces are denoted B and A in Figure 1, a terminology used in a previous paper.[4] Using an obvious analogy, the corresponding faces were later described[7] *as the "five" and "four" faces of dice* (cf. Figure 2). The situation is symmetrical for left-handed helices: residues 2′ and 3′ are exposed when observed along the $-b$ direction; residue 1′ alone is exposed when observed along the $+b$ direction.

As a result, both helical hand and surface structures alternate in successive (040) planes when observed from either the $+b$- or $-b$-axis direction (Figure 1, left and right sides).

The helical hand can be determined provided the a- and c-axis orientations are known. As illustrated in better detail in Figure 2b, two neighbor methyl groups *materialize* the underlying helical path in contact faces where they are both exposed ("five" faces). This helical path is parallel to the [101] direction, i.e., to the *short* diagonal of the lozenge-shaped *ac* plane (Figure 2b). Figure 2a represents a face with single methyl groups exposed ("four" faces). It would, by itself, be insufficient to indicate the helical

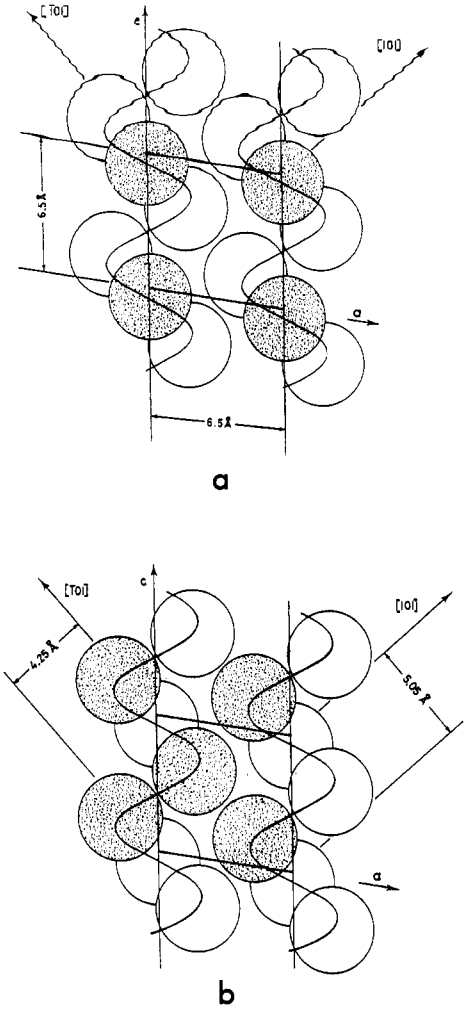

Figure 2. Large-scale view of the two possible contact faces B and A with indications of dimensions. In both figures, two helices of the contact plane are imaged. Note the striking difference in density of exposed methyl groups (shaded). The two patterns can be described as the "four" (a) and "five" (b) patterns of dice (simple and face centered, respectively).[7]

path. However, it is apparent that the underlying path is roughly parallel to [101], i.e., to the *long* diagonal of the lozenge-shaped *ac* face of the unit cell.

The orientations of the *a* and *c* axes are easily determined by diffraction techniques. Morphological determination of these orientations in α-iPP is also possible thanks to the peculiar homoepitaxy or rotation twin leading to quadrite formation (ref 18 and 19 and cf. later Figure 4). This homoepitaxy results in two populations of lamellae at $\simeq$100° to one another in which the *c* (chain) axis of one set of lamellae is parallel to the *a* axis of the other set. Since the chain axis is normal (or nearly so) to the lamellar end surface, the determination of *a*- and *c*-axis orientation and, as a consequence, of helix chirality in each set of lamellae is straightforward (cf. Figure 4 later and legend to Figure 9 in ref 4 for further details).

The γ phase of isotactic polypropylene has essentially the same structure based on layers of isochiral helices as the α phase. In the γ phase, however, the rotation twin axis which creates α-phase quadrites is integrated as an *element of symmetry of the unit cell.* As a result, *the structure is made of bilayers of chains with chain axes inclined at 80 or 100°.*[20] The unit cell is orthorhombic with parameters a = 8.54 Å, b = 9.93 Å, and c = 42.41 Å and the chain axes are parallel to the two diagonals of the *ab* plane. The strict alternation of layers of parallel right-handed (R) and left-handed (L) helices—RLRLRL...— of the α phase becomes in the γ phase RRLLRRLL... where antichiral chains in neighboring layers have parallel axes and isochiral ones are tilted at 80 or 100° (cf. Figure 5c). In this structure with nonparallel chain axes, the lamellar end surface $(010)_\gamma$ plays a symmetric role for the two chain orientations: it is parallel to the (101) plane of the α phase, i.e., to one bisector of the quadrite structure (cf. Figure 5d).[5,6,21] The surface structures of the lateral faces (001) are essentially identical to those of the α phase, with alternation of a single and of two methyl group surfaces ("four" and "five" faces).

The challenge of a complete structure elucidation of epitaxially crystallized iPP therefore implies identification of two populations of α-phase crystals, one population of γ-phase, two orientations of chain axes (different for each of the two populations of α-phase lamellae but both present in any γ-phase lamella), and, finally, discrimination (by AFM) between two lateral planes with different methyl group densities at the outermost surface and determination of the hand of the exposed helices.

Results

The structure of epitaxially crystallized iPP as established by electron microscopy and electron diffraction is described first. This presentation makes reading of the present paper self-contained and helps set the stage for the AFM work described next.

1. Electron Microscopic Investigations of Thin Epitaxially Crystallized iPP Films. (a) Structure of the Thin Films. Figure 3a illustrates the morphology of thin films of high molecular weight iPP crystallized in the *α phase* on benzoic acid, as revealed by Pt/C shadowing. Figure 3b is a diffraction pattern in proper relative orientation. Figure 3c is a similar pattern, taken with a larger camera length, of a gold-decorated film. These three micrographs provide the basic information needed for a complete structural characterization as represented in schematic form in Figure 4:

(i) The cross-hatched morphology of iPP lamellae standing on edge is very reminiscent of that of solution-grown quadrites and suggests two chain orientations with a similar relationship.

(ii) The wide-angle diffraction pattern confirms that the *ac* face of α-iPP is exposed: the structure is seen along the (+ or −) *b*-axis direction, as in Figures 1 and 2; the [101] direction (vertical) is parallel to the acute angle of the lamellae.

(iii) The combined wide- and low-angle diffraction pattern of Figure 3c confirms that the helix axes are nearly normal to the lamellar surfaces, and lamellar thickness is $\simeq$13 nm.

(iv) Since the *a* and *c* orientations are known in both sets of lamellae, it is possible to determine the hand and setting of all helices in the structure (Figure 4). Keeping in mind that, for helices with two methyls facing the observer, the bisector of the acute angle made by the lamellae corresponds to the helical path and knowing the helix axis orientation, it follows at once that these helices are right-handed in lamellae oriented to the upper right (shaded) and left-handed in lamellae oriented to the upper left (unshaded) (cf. Figure 4, bottom). From the crystal structure, it also follows that helices of the next layer with one methyl group facing the observer have opposite chiralities (Figure 4, middle).

Figure 5a represents a gold-decorated, epitaxially crystallized thin film of *mixed α and γ phases* obtained with the low molecular weight, vaporized iPP material, with the same orientation as Figure 3a. As opposed to the

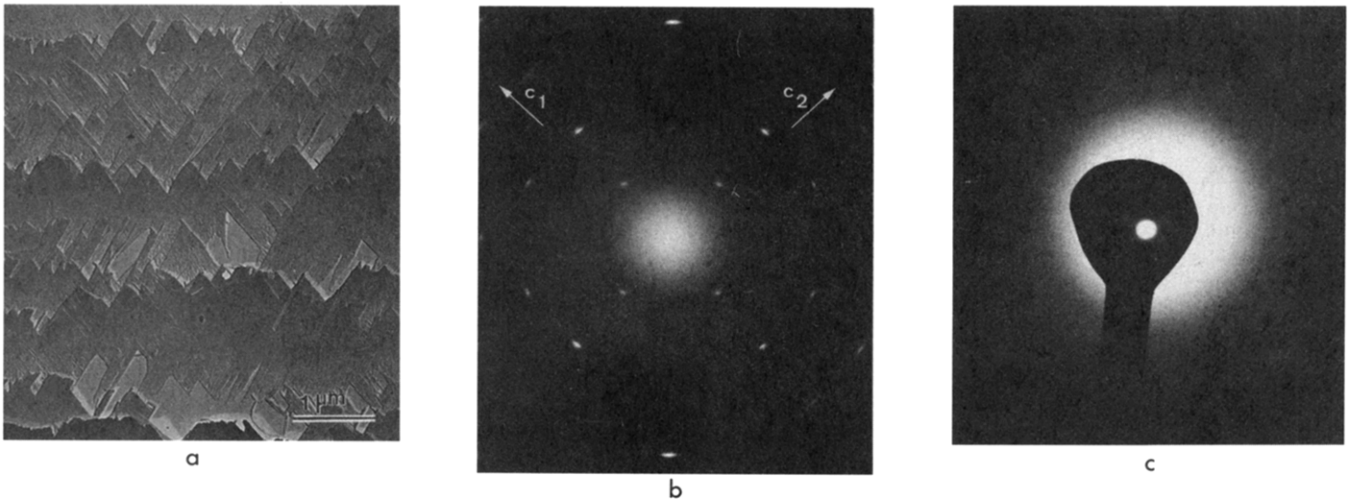

Figure 3. (a) Lamellar structure of the contact face of α-iPP with benzoic or nicotinic acid after dissolution of the substrate. The exposed contact face has been shadowed with Pt/C. Note the existence of two lamellar orientations, very reminiscent of the structure of iPP "quadrites"[18] formed on solution crystallization. (b) Selected-area electron diffraction (wide angle) of an area as in (a) in proper relative orienation. This pattern indicates two chain orientations at 80° (or 100°) to each other: the four inner 110 spots (6.4-Å^{-1} spacing) correspond to two equators; the unit cells are seen in *b*-axis projection. (c) Selected-area electron diffraction pattern (wide and low angle) of a film as in (a) but decorated with gold particles (gold decoration[23]). The wide-angle pattern is taken first while using a beam stop (four outer 110 spots corresponding to the inner ones of (b)). A second exposure (in the area of the photographic plate covered by the beam stop) is used to record the low-angle pattern of the lamellar structure. This second pattern is taken using a larger camera length: the wide- and low-angle patterns are not therefore on the same scale but are in proper relative orientation.

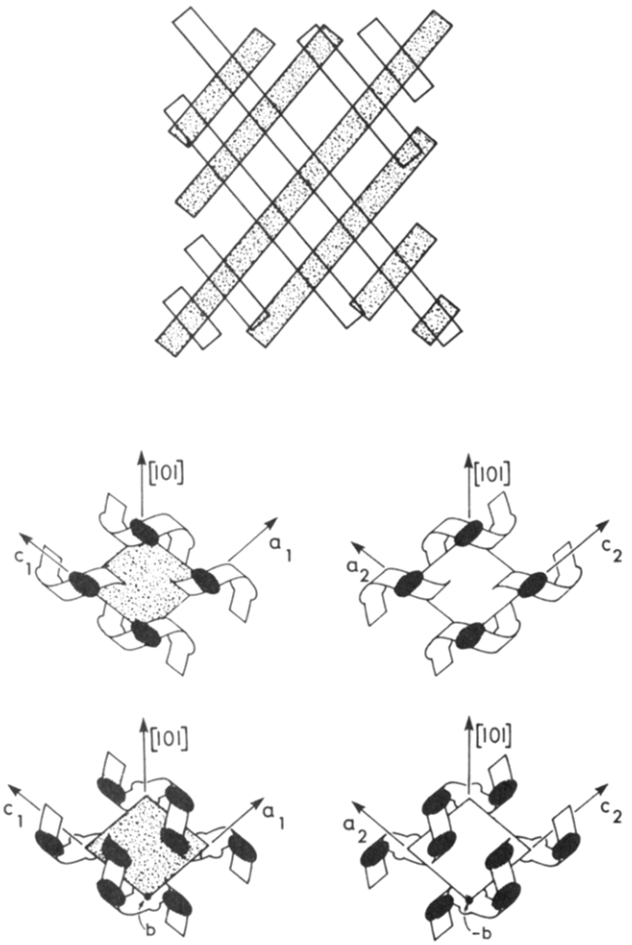

Figure 4. Schematic representation of the structure of epitaxially crystallized α-phase iPP with indication of hand of helices in the two sets of lamellae (shown as shaded and white).

morphology in that figure, a significant portion of the film is made of γ-phase lamellae oriented parallel to the bisector of the acute angle made by relatively few α-phase lamellae. In this projection, mixed α- and (mainly) γ-phase films have a diffraction pattern (Figure 5b) very similar to that of pure α-phase films. Furthermore, in view of the peculiar γ-phase structure, *each and every γ-phase lamella* is built up with *all four populations of layers* schematized in Figure 4 for the two *distinct* populations of α lamellae. The structural lamellar and chain orientations and unit cell orientations in such mixed α- and γ-phase films are schematized in Figure 5d.

(b) Epitaxy and Contact Planes. The diffraction evidence underlines the importance of the (010) contact faces of α-iPP and of the structurally equivalent (001) faces of γ-iPP. The epitaxial relationship is based on matching of polymer and substrate lattice periodicities. In the present case, the (101) α planes (with an interplanar 5.05-Å periodicity) and/or (020) γ planes (4.97-Å periodicity) match the substrate 5.14-Å *b*-axis periodicity, i.e., the interrow distances of benzoic acid molecules.

Diffraction evidence cannot go beyond this analysis. In particular, *diffraction does not tell which one of the "four" or the "five" faces represented in Figure 2 is the contact plane* since only the *orientation of the unit cell* can be determined.

The nature of this contact plane is thus open to conjecture. It must be guessed after the scheme of polymer–substrate interactions that appears a priori more favorable. In previous papers,[3,4] this guess favored the more densely populated face shown in Figure 2b. This preference was based on the structural resemblance of PE chains and the rows of methyl groups in α-iPP. These rows are parallel to the [101] direction of iPP, which is at 50° to the helix axis, and therefore straddle many helices. Indeed, upon epitaxial crystallization, both the [101] direction of α-iPP and the chain axis of PE align parallel to the *a* axis of the benzoic acid substrate.[3] However, *this scheme is only one out of two alternatives and is not, so far, supported by experimental evidence.* AFM imaging of the contact interface should help provide those experimental evidences.

2. Atomic Force Microscopy of the Contact Faces of iPP, α Phase. The visualization of contact faces involves low- and high-magnification pictures. The latter are Fourier transformed and filtered before reconstruction. As these manipulations may cast doubt on the final results,

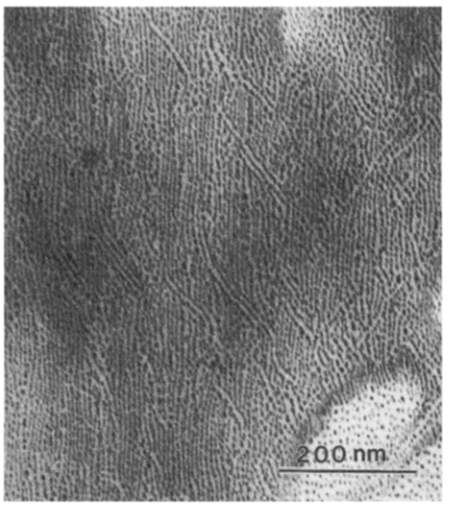

a

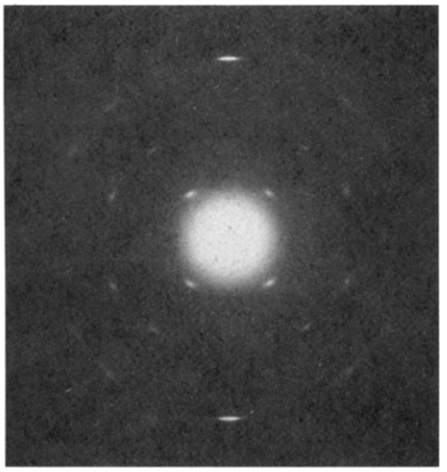

b

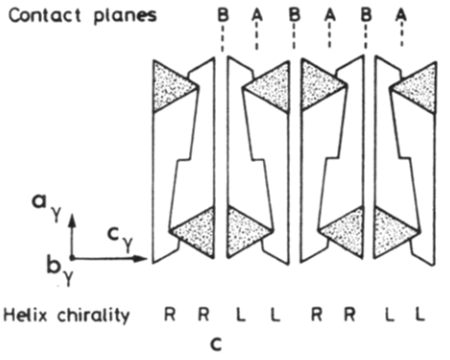

c

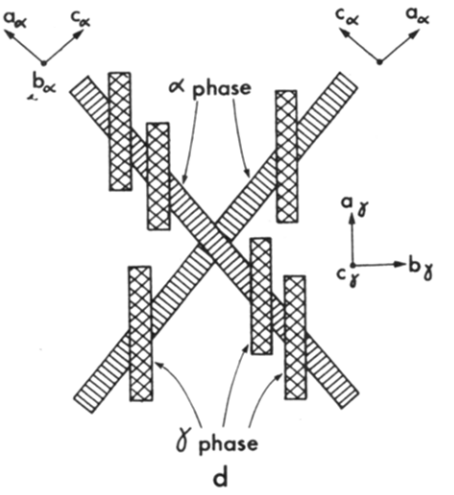

d

Figure 5. (a) Electron micrograph of an epitaxially crystallized film of iPP with mixed α and γ phases. Note the two orientations at 80° of the few α-phase lamellae and the unique orientation of γ-phase lamellae parallel to the [101] α-phase direction (vertical). (b) Electron diffraction pattern of a film as in (a). Note overall similarity of this pattern and that of pure α phase[20] (Figure 3b). The four inner reflections are 111_γ; a_γ vertical, b_γ horizontal. (c) Model of chain arrangement in γ-phase crystal structure as determined by Brückner and Meille,[20] seen along the b_γ axis (normal to lamellar surface). Note that chains are parallel and antichiral, and at 80° and isochiral, when contacting through the B and A faces, respectively. (d) Lamellar and chain axis orientations in the composite α- and γ-phase epitaxially crystallized film in (a). Note that the two chain orientations found in combination in γ-phase lamellae are parallel to those existing, separately, in the α-phase lamellae (from ref 6).

special care has been taken to evaluate the impact of our sampling and filtering techniques. Several representative figures will illustrate that impact.

(a) Lamellar Structure. *Large-scale views* of the epitaxially formed films of high molecular weight, α-phase iPP display a very clear array of parallel ridges (Figure 6) with a periodicity of $\simeq$13 nm. Similarities of this figure and the electron micrograph of Figure 3a are striking: the AFM picture clearly represents a small film area with parallel lamellae, i.e., has sampled one out of the two populations of lamellae.

The lamellar structure is detected because the interlamellar material forms *protrusions* on the surface—actually only 0.4 Å or less above the neighbor crystal core of the lamellae.

Such "ridging" or "bulging" of the interlamellar material is surprising, since the polymer crystallizes at T_c on a molecularly smooth crystal substrate. We suggest therefore that this bulging occurs as a result of cooling from T_c to room temperature. During this $\simeq$100 °C temperature drop, both benzoic acid and the support cover glass of the polymer film experience thermal contraction. The cubic expansion coefficient is $\simeq 3 \times 10^{-4}$/°C for organic crystals and glasses, and the linear expansion coefficient is $\simeq 1 \times 10^{-4}$/°C: for the $\simeq$100 °C drop to room temperature, the support glass contracts by $\simeq$1%. Contrary to glasses, the thermal expansion coefficients of crystalline polymers are highly asymmetric; in particular, they are zero or even negative along the helix axis. As a result, contraction of the glass in the polymer chain axis direction must be accommodated mainly by the interlamellar material of the polymer film. This effect is small but can be detected in the present films thanks to their unusual morphology (oriented, edge-on lamellae) and to the AFM high z-axis sensitivity. In the context of this investigation, this feature turns out to be of major importance for crystal phase determination and assessment of helical hand.

(b) Methyl Group Pattern. A higher magnification AFM picture which represents an area 17 × 17 nm is shown in Figure 7a. As is natural, reduction on reproduction and black and white representation do not do full justice to the information content of the original false color picture in which several areas with dots in a lozenge pattern can be clearly discerned.

The essential features of this picture are revealed by Fourier transform. The 2D transform is represented in

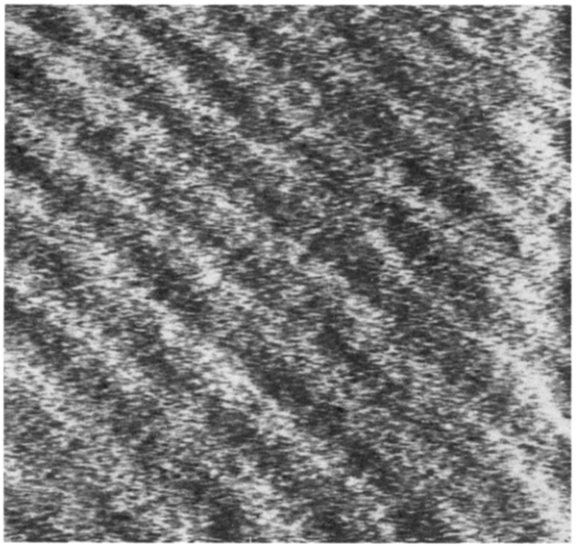

Figure 6. Low-resolution AFM picture of the lamellar structure in epitaxially crystallized α-phase iPP. The imaged area comprises only one of the two possible orientations of lamellae (displayed in Figure 3a).

Figure 7b; it is characterized by two pairs of strong spots (marked 1 and 2) corresponding to reciprocal distances of $\simeq$6.5 Å and by two sets of spots (marked 3 and 4) in one direction only (vertical). This asymmetry of the pattern reflects instrumental features of the AFM technique. In this horizontal scanning direction, stick-slip with the AFM is exerted at each atomic (here methyl group) site. The force built up at the site suddenly relaxes as the tip slips to the next site: resolution in this horizontal direction is not expected to be superior to the methyl group periodicity. In the vertical direction, however, resolution can be higher since scan lines are less than 1 Å apart.

Filtering and back Fourier transform of the pattern illustrate these features (Figure 8). As can be expected, selection of the four central spots (i.e., 1 and 2) yields a rather featureless, nearly square pattern of dots (Figure 8a). Selection of all the spots in Figure 7b yields a picture where interference of the scanning probe periodicity becomes perceptible (Figure 8b). Selection of the six inner spots yields the most illustrative and "reasonable" picture of the surface structure, which is enlarged in Figure 9. It represents a lozenge-shaped array of protrusions (light areas) with a slightly elliptic shape linked with the lower resolution (of mechanical origin) in the scanning direction.

Figure 9 is clearly a picture with submolecular resolution of the polymer contact surface. The protrusions are $\simeq$6.9 and 6.5 Å away in two rows $\simeq$95–100° apart. Both distances and angles correspond to the pattern of methyl side chains illustrated in Figure 2a. *AFM pictures therefore provide an unambiguous answer to the "contact surface issue"*: this surface contains the *lower density of methyl groups* (the "four" face) and not, as initially considered, the higher one (the "five" face).

(c) Crystal Phase and Helical Hand. Due to its lozenge symmetry, the pattern of methyl groups does not, by itself, provide any additional information and *does not*, in particular, differentiate rows of methyl groups belonging to the same helical stem from rows of methyl groups in different stems. However, combining lamellar and methyl group patterns resolved in the low- and high-magnification pictures enables recognition of the crystal phase and helix orientation and chirality.

The α crystal phase is *identified* by its characteristic (near) right-angle orientation of the lamellar fold surface

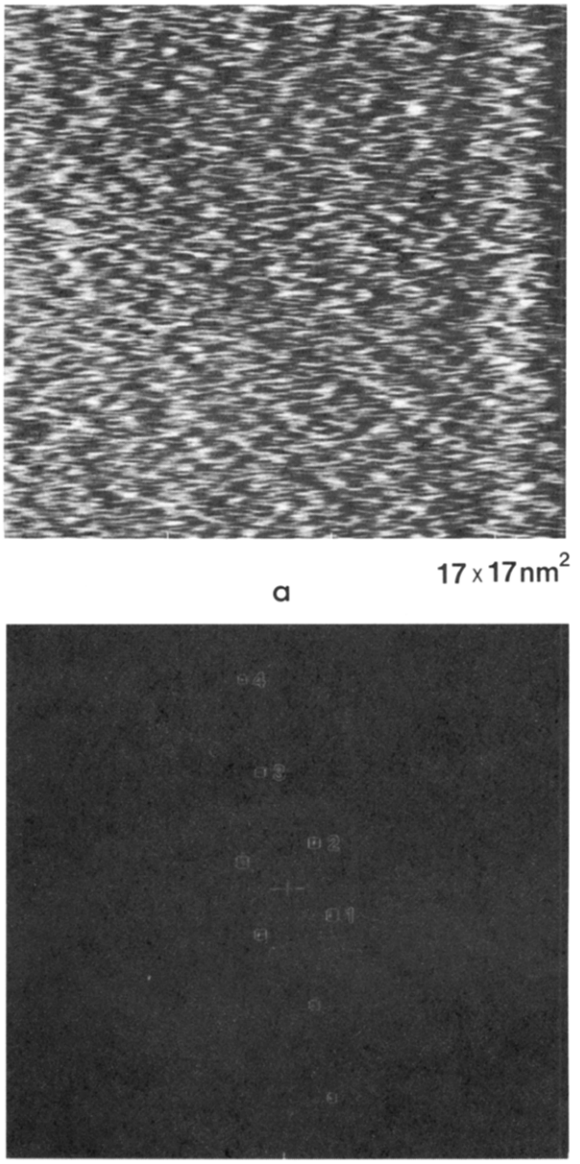

Figure 7. (a) Unfiltered AFM image of a 17 × 17 nm area selected in Figure 6a. (b) Fourier transform of (a) composed of four pairs of spots, marked 1–4. Note that the four central spots, although similar to those of Figure 3b, refer here to the *surface* structure of an area with a *single* chain orientation, whereas Figure 3b represents the first equatorial diffraction spots (110) for two *different* chain orientations.

(cf. Figure 6a) and one row of methyl groups in Figure 9. This is the case for *methyl groups aligned from the lower left to upper right* of Figure 9. *These methyl groups belong therefore to the same helix stem*, and *the crystal phase is* α.

The helix chirality follows from the above: in Figure 9, the second set of rows of methyl groups, from the lower right to upper left, *materializes the a-axis orientation*; i.e., methyl groups in these rows belong to different helices.

From the discussion on helix chirality (Figure 2a), the underlying helix path is parallel to the long diagonal of the lozenge pattern. Combined with helix axis orientation, it follows that *helices exposed in Figure 9 are right-handed* (cf. Figure 4, center right, for a nearly similar situation). It is clear, however, that in other areas of the sample, the exposed helices may be left-handed. These areas would correspond to the differently oriented set of lamellae in the quadrite (cf. Figure 4). The AFM experimental

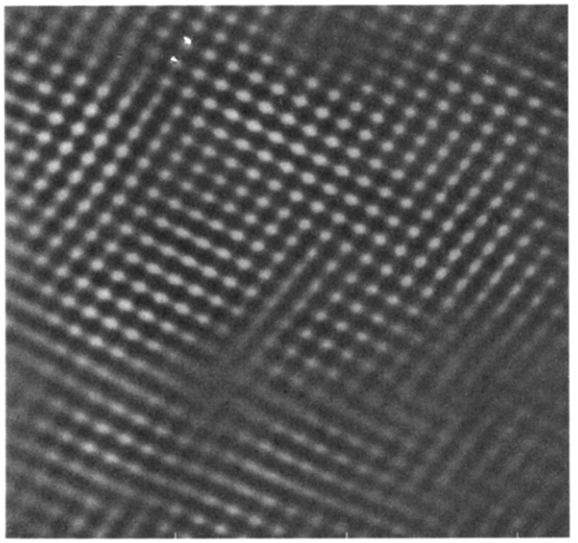

Figure 8. Fourier-filtered images of Figure 7a using diffraction spots marked (a) 1 and 2 and (b) 1–4 in Figure 7b.

evidence would be as follows: the high-resolution picture (Figure 9) would be identical, but the orientation of lamellae in low resolution would be nearly at right angles to that displayed in Figure 6a. This would identify the lower right to upper left row of methyl groups as parallel to the helix axis. It is easy to convince oneself that the exposed helices would be left-handed (cf. also Figure 4). This point is discussed in some detail because an unfortunate formulation in the summary to ref 7 may have been interpreted to mean that *all* helices exposed in the contact plane are right-handed. That statement referred only to the area pictured in Figures 6a and 9.

As examined now, however, a structural identification in similar detail turns out to be impossible for the γ phase.

3. Atomic Force Microscopy of the Contact Faces of iPP, γ Phase. (a) Lamellar Orientation and Crystal Phase Identification. The images in Figure 10 represent the low- (Figure 10a) and high-resolution (Figure 10b) pictures (the latter, after Fourier transform and filtering) of the contact surface of epitaxially crystallized low molecular weight iPP film. The lamellar structure and the by now familiar lozenge-shaped pattern of light dots

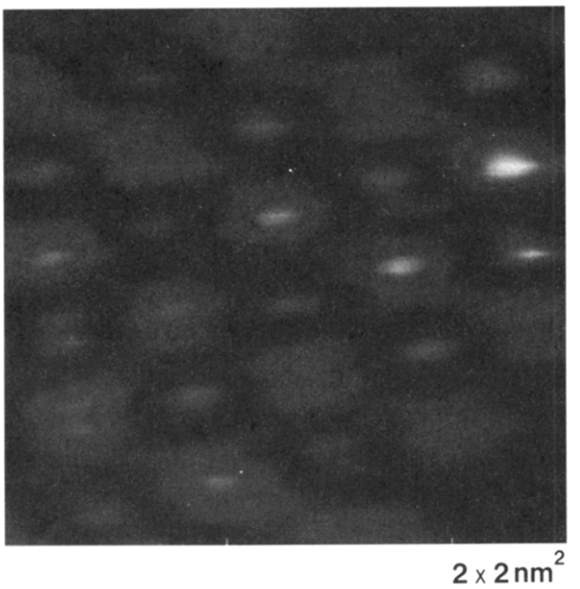

Figure 9. Enlarged Fourier-filtered image of Figure 7a using diffraction spots marked 1, 2, and 3 in Figure 7b. Note the simple, lozenge-type pattern and horizontal elongation of peaks corresponding to the methyl groups (darker areas).

corresponding to methyl groups are very similar to those of the α-phase one. However, a striking difference with the corresponding previous figures lies in the relative lamellar and methyl row orientations. *The lamellar surface is now inclined at 50° to both rows of methyl groups* rather than being perpendicular to one of them. The pattern of methyl groups similar to the α-phase structure and its different orientation relative to the lamellar surface are major characteristics of and *identify the γ phase.*

(b) Contact Face Issue. Given the structural identity of layers of helices in α- and γ-phase iPP, it is not surprising that the same "contact surface structure" determined for the α phase is also found for the γ phase. Clearly, epitaxy selects the same type of iPP contact surfaces in both phases, i.e., $(001)_\gamma$ with the "four" methyl group pattern.

(c) Helical Hand Issue in the γ Phase. Whereas the epitaxies of the α and γ phases are similar in every respect, the structural analysis cannot go beyond recognition of the γ phase. In particular, *determination of the helix hand is not possible for the γ-phase.* This impossibility stems from the symmetrical disposition of the rows of methyl groups relative to the lamellar surface. *No morphological criterion* as exists for the α phase (orthogonality of lamellar surface and one row of methyl groups) *is available to decide which one of the two rows of methyl groups corresponds to the chain axis direction in the exposed γ-phase $(001)_\gamma$ plane.* It is only possible to give the two terms of the alternative regarding helix chirality. Applying the reasoning developed for the α phase, the exposed helices are left-handed if the row of methyl groups oriented at 10 o'clock corresponds to the helix axis and right-handed if oriented at 2 o'clock in Figure 10b. (Note, however, that helical hand in γ-phase lamellae can be determined when their branching onto α-phase ones is identified, as the sequence of helical hands determined in those α-phase crystals can be carried over to the γ-phase ones.[6])

Discussion

1. AFM of Epitaxially Crystallized Films. The unusually clear answer given by AFM about contact surface in epitaxially crystallized iPP is aided by (i) the detailed

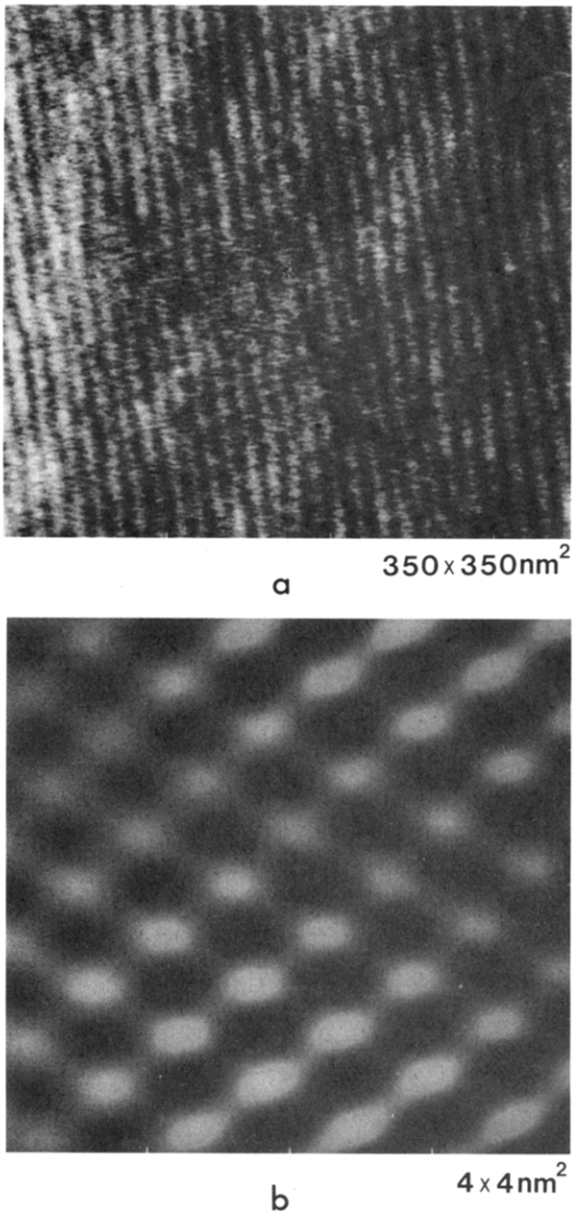

Figure 10. (a) Low-resolution image of the lamellar structure in γ-phase iPP films epitaxially crystallized on benzoic acid. (b) Fourier-filtered image of the methyl group pattern in an area as in (a) in proper relative orientation. Note the pattern of methyl groups similar to that of the α phase but the different orientation relative to the lamellae, which identifies the γ phase.

understanding of the iPP α-phase[14–16] and, more recently, γ-phase structure,[6,20–22] morphological characterization of lamellar branching, analysis of the underlying molecular origin, and recognition of helical hand from simple morphological evidence[4] and (ii) two favorable features of epitaxial crystallization: (a) formation of a "molecularly flat" surface of the polymer (this planarity reflects the habit of the substrate crystal; it is at variance with most "spontaneous" bulk polymer morphologies which are not smooth on the same scale) and (b) formation of a regular pattern in a single crystallographic plane extending uniformly over large areas of the former substrate crystal, since the favorable local epitaxial relationship is reproduced throughout the contact surface.

2. Contact Faces and Helix Hand. The first outcome of this study is the possibility to image the organization of epitaxially crystallized edge-on lamellae, in spite of their being formed at T_c, on a "molecularly smooth" substrate surface.

The second and main objective of this work has been recognition of the exact contact surface structure out of two alternate candidates. *For AFM purposes, the two surfaces are "ideally different"*, since they differ *by their symmetry*. Even if the unfiltered image does not reveal strikingly the pattern of methyl groups, its Fourier transform is very telling as regards the symmetry of this pattern. In particular, the four inner spots of Figure 7b with spacing 6.5 Å^{-1} would be very faint or absent if the "five" faces were imaged.

The possibility to *correlate lamellar and lattice orientation* makes it possible to determine the *crystal phase*, α or γ, or iPP. The pattern of methyl groups imaged by AFM does not differentiate methyl groups that belong to a single helix, but for the α phase only the helix orientation can be determined with the help of morphological indicators—here the lamellar orientation. The *a*-axis orientation can then be read directly from the pictures and the helical hand can be determined from the known α-phase crystal structure.

The helix hand determination from AFM pictures of α-iPP may—rightly—appear as fairly involved. For the main part, the complications stem from the highly exceptional symmmetry of the contact face and near identiity of the *a* and *c* parameters of the unit cell. Fortunately, most other polyolefins or, for that matter, most helical polymers with longer side chains should be easier to deal with: the outside atoms, which materialize the helical path, and the lower symmetry of the contact faces should provide sufficient clues to directly read helical hands on AFM pictures.

3. Contact Faces in α-Phase Epitaxy and Homoepitaxy and γ-Phase Crystal Structure. Determination of the contact surface structure by AFM techniques provides new clues on iPP epitaxy and homoepitaxy and γ-phase crystal structure.

(a) Visualization of the contact surface helps elucidate α-iPP/low molecular weight organic substrate epitaxy. As already indicated, a fairly "flat" contact surface was previously favored, i.e., the "five" face with its rows of methyl groups parallel to [101] since they mimic PE chains which also epitaxially crystallize on those same substrate.[3] On the contrary, AFM results indicate that a "hilly" surface of methyl groups interacts deeply with the substrate. Note in this context that energy analysis would be hardly tractable in modeling this epitaxy of dimensionally ill-matched contact surfaces of different materials.

(b) α-Phase lamellar branching and the γ-phase structure also rest on epitaxial interactions of the α-phase (010) plane. The homoepitaxy is favored by a near-perfect lattice match and by the similar nature of the two faces (3_1 iPP helices). The initial structural analysis of iPP quadrites[4] could not decide between the two possible contact surfaces (the "four" or "five" pattern of methyl groups). However, structure determination of the γ-phase structure showed that *the homoepitaxy involves the "four" faces, i.e., the same contact faces as in the present iPP/benzoic acid epitaxy*.[20,21] Furthermore, repetition of this packing scheme in γ-iPP suggests that it is energetically favored over the more classical parallel alignment of chains. Evaluation of the interaction energies in α- or γ-iPP for epitaxial and parallel orientation of chains does not, however, reveal any significant differences (Colonna-Cesari and Lotz (unpublished) and ref 22). It is of interest to note that both homoepitaxy (in α lamellar branching and its systematization in the γ phase) and heteroepitaxy on benzoic and nicotinic acid involve the same contact plane, which appears therefore energetically favored in

spite of inconclusive (but not opposite) energy analysis results.

Conclusion

AFM is of invaluable help in the concerted structural characterization of epitaxially crystallized thin films of isotactic polypropylene (α and γ phases) by electron microscopy, electron diffraction, and atomic force microscopy. Low-magnification AFM pictures reveal the lamellar organization, probably through bulging of the interlamellar phase on cooling to room temperature. High-magnification AFM pictures help determine the contact face structure, information beyond reach of electron microscopy and electron diffraction techniques. Specifically, they indicate that the contact face with a low density of methyl side chains is preferred over the alternate face with a higher density of methyl groups. This same contact face is involved in the γ-phase structure and, by inference, in the α-phase homoepitaxy. Preference for one face (the "four" face) demonstrated by AFM therefore opens the way for a molecular and submolecular understanding of polymer epitaxy. For the specific iPP case, work is in progress to establish whether modification of the substrate structure, or even nature (e.g., use of alkali halides rather than aromatic acids), is sufficient to favor the alternate "five" face as a contact plane.

References and Notes

(1) Binnig, G.; Rohrer, H.; Gerber, Ch.; Weibel, E. *Phys. Rev. Lett.* **1982**, *49*, 52.
(2) Stocker, W.; Bar, G.; Kunz, M.; Möller, M.; Magonov, S. N.; Cantow, H.-J. *Polym. Bull.* **1991**, *26*, 215.
(3) Wittmann, J. C.; Lotz, B. *Prog. Polym. Sci.* **1990**, *15*, 909.
(4) Lotz, B.; Wittmann, J. C. *J. Polym. Sci., Polym. Phys. Ed.* **1986**, *24*, 1541.
(5) Lotz, B.; Graff, S.; Wittmann, J. C. *J. Polym. Sci., B: Polym. Phys.* **1986**, *24*, 2017.
(6) Lotz, B.; Graff, S.; Straupé, C.; Wittmann, J. C. *Polymer* **1991**, *32*, 2902.
(7) Lotz, B.; Wittmann, J. C.; Stocker, W.; Magonov, S. N.; Cantow, H.-J. *Polym. Bull.* **1991**, *26*, 209.
(8) Dorset, D. L. *Chemtracts: Macromol. Chem.* **1992**, *3*, 200.
(9) Fillon, B. Thesis, Université Louis Pasteur, Strasbourg, 1989.
(10) Fillon, B.; Wittmann, J. C.; Lotz, B.; Thierry, A. *J. Polym. Sci., Polym. Phys. Ed.* **1993**, 1383–1393.
(11) Fillon, B.; Lotz, B.; Thierry, A.; Wittmann, J. C. *J. Polym. Sci., Polym. Phys. Ed.* **1993**, 1395–1405.
(12) Fillon, B.; Thierry, A.; Wittmann, J. C.; Lotz, B. *J. Polym. Sci., Polym. Phys. Ed.* **1993**, 1407–1424.
(13) Ashida, M.; Ueda, Y.; Watanabe, T. *J. Polym. Sci., Polym. Phys. Ed.* **1978**, *16*, 179.
(14) Natta, G.; Corradini, P. *Nuovo Cimento, Suppl.* **1960**, *15*, 40.
(15) Mencik, Z. *J. Macromol. Sci.* **1972**, *B6*, 101.
(16) Hikosaka, M.; Seto, J. *Polym. J.* **1973**, *5*, 111.
(17) Natta, G.; Corradini, P.; Bassi, I. W. *Nuovo Cimento, Suppl.* **1960**, *15*, 52.
(18) Khoury, F. *J. Res. Natl. Bur. Stand., Sect. A* **1966**, *70A*, 29.
(19) Padden, F. J., Jr.; Keith, H. D. *J. Appl. Phys.* **1966**, *37*, 4013.
(20) Brückner, S.; Meille, S. V. *Nature* **1989**, *340*, 455.
(21) Meille, S. V.; Brückner, S.; Porzio, W. *Macromolecules* **1990**, *23*, 4114.
(22) Ferro, D. R.; Brückner, S.; Meille, S. V.; Ragazzi, M. *Macromolecules* **1992**, *25*, 5231.
(23) Bassett, G. A. *Philos. Mag.* **1958**, *3*, 1042.